Fluid Antenna Port Selection in Underlay Cognitive Radio Networks

Hui Zhao and Dirk Slock
Communication Systems Department, EURECOM, Sophia Antipolis, France
Email: hui.zhao@eurecom.fr; dirk.slock@eurecom.fr

***Abstract*—We study fluid antenna (FA) port selection in underlay cognitive radio (CR) networks, where a single FA-enabled secondary transmitter serves a single-antenna secondary receiver under the underlay CR mechanism that caps the interference at the primary user via instantaneous power control. For each FA port, we formalize the resulting signal-to-noise ratio (SNR) and propose a CR-aware selection rule that prioritizes ports offering a favorable balance between the secondary-link gain and the power-control link to the primary user. This contrasts with the conventional main-channel maximization (MCM) rule, which ignores the power-control link imposed by underlay CR—a choice often adopted in non-CR scenarios. Through rigorous mathematical derivations, we establish the exact diversity orders of both FA policies and show that each attains a diversity order equal to the rank of the FA port correlation matrix. For comparison, we further consider a traditional multi-antenna transmitter employing maximum-ratio transmission under the same underlay constraint and prove that its diversity order equals the number of transmit antennas. Monte Carlo simulations over Rayleigh fading channels validate the analysis, demonstrating sizable outage gains of the proposed CR-aware selection over MCM, and performance comparable to that of traditional multi-antenna transmission.**

I. Introduction

Fluid antenna (FA) realizes a position-agile radiator whose active port can hop among many closely spaced locations inside a tiny aperture. Shifting the port by only a small fraction of a wavelength reshapes the local fading pattern, allowing opportunistic port probing to escape deep fades—even when the channels across ports are strongly correlated—while keeping the device footprint and radio frequency (RF) front-end count minimal [1]. Recent surveys and preliminaries outline practical embodiments using liquid-metal radiators, reconfigurable pixel arrays, and mechanically actuated structures, highlighting their suitability for handset-class form factors [2], [3]. Reported prototypes further indicate near-term feasibility, positioning FA as a compact and adaptable building block for future wireless communications [4].

As FAs move from concept to deployment, they will increasingly operate in bands where dynamic spectrum sharing with incumbents is the norm—precisely the settings governed by cognitive radio (CR) frameworks [5]. Surveys of CR highlight its role as a practical response to spectrum scarcity and under-utilization, with broad prospects across heterogeneous networks and IoT-heavy environments [6], [7]. Therefore, recent work has begun to connect FAs with CR functions by using port agility to strengthen spectrum sensing (e.g., [8], [9]), underscoring a natural synergy between FA capabilities and CR requirements. Taken together, these trends suggest that future FA designs should be inherently CR-aware: port selection and power control need to account for primary user (PU) protection, so that FA gains can be realized without compromising licensed users.

Consider that FAs are deployed in the secondary user (SU) of a commonplace underlay CR system, where the interference power at the PU should be less than a threshold to protect the quality-of-service (QoS) of the primary network [10]–[12]. A natural question arises: *should FA port selection simply reuse the non-CR rule that maximizes the instantaneous secondary-link gain, or should it be redesigned to account for the SU power control mandated by underlay CR?* Because the SU's transmit power is continually shaped by the interference path toward the primary receiver, the effective link quality depends jointly on the SU link and the power-control link. This motivates a *CR-aware FA port selection* strategy that couples port choice with the underlay power-control mechanism, with the goal of surpassing the performance of the conventional non-CR selection rule.

A key challenge in analyzing FA performance is that FA ports are packed within a tiny aperture, so the channels observed across ports are strongly correlated. This high correlation undermines many standard independence-based tools and makes performance analysis unusually hard. For point-to-point (P2P) links, [1] derived the first exact outage probability (OP) expression, but only in a heavy integral form that is difficult to evaluate and offers little intuition—most notably, it does not reveal the exact *diversity order*, a central indicator of reliability in communication systems. Subsequent works (e.g., [13]–[15]) proposed various approximations and provided diversity order estimates, yet a rigorous exact value remained elusive. Our most recent study [16] introduced a novel method that, for the first time, rigorously proves the P2P diversity order and gives a remarkably simple approximation for the OP. However, all of these results pertain to non-CR settings. Once underlay CR is introduced, the transmit-side power control couples the secondary link

This work was supported in part by EURECOM's industrial members: ORANGE, BMW, SAP, iABG, Norton LifeLock, in part by the French projects EEMW4FIX and PERSEUS (PEPR-5G), and in part by the Huawei France-funded Chair towards Future Wireless Networks.

with the power-control link to the primary network, further complicating the analysis. As a result, rigorous studies of FA performance in CR networks are scarce.

In this paper, we consider a FA-enabled secondary transmitter in underlay CR networks, and we: (i) introduce a CR-aware port selection rule that couples port choice with the underlay CR power-control mechanism, and analytically show it dominates the conventional non-CR selection based solely on the secondary link; (ii) through rigorous derivations, establish that for both CR-aware selection and non-CR selection over correlated Rayleigh fading channels, the diversity order equals the rank of the FA port channel correlation matrix; (iii) analyze a traditional multi-antenna transmitter with maximum-ratio transmission (MRT) under the same underlay constraint as a benchmark, and prove that its diversity order equals the number of transmit antennas; and (iv) provide simulations that corroborate the analysis, demonstrating sizable outage gains over the non-CR baseline and the conventional multi-antenna transmission.

Paper Structure: Section II details the underlay CR system model, including CR power control, received SNR expressions, the proposed CR-aware FA port selection, the non-CR selection baseline, and a traditional multi-antenna benchmark. Section III develops the analytical framework and establishes the diversity orders of the considered schemes. Section IV presents numerical results under the Jake's correlation model and discusses trends with respect to system parameters of interest. Section V concludes the paper with key findings and design insights.[1]

II. System Model

We consider an underlay CR network comprising a single FA-enabled secondary transmitter (SU-Tx) communicating with a single-antenna secondary receiver (SU-Rx) while coexisting with a licensed PU. The SU opportunistically accesses the primary spectrum under an interference constraint at the PU to guarantee the PU's QoS. The interference threshold at the PU is denoted by I_{th}. We adopt the common FA architecture with N discrete ports uniformly distributed across the aperture and fed by a single RF chain, so that in each transmission round exactly one port is activated to deliver the signal (cf. [2], [13], [15]). We model the wireless channel as Rayleigh fading. The transmit symbol s has unit average power, and the additive white Gaussian noise (AWGN) at the SU-Rx is circularly symmetric complex Gaussian with variance N_0.

Let $h_{\mathrm{P},n}$ denote the complex channel coefficient from the n-th FA port of the SU-Tx to the PU, encompassing large-scale path loss and small-scale fading. When the n-th port is active, the instantaneous interference power received at the PU is of the form $I_n = P_{T,n}|h_{\mathrm{P},n}|^2$, where $P_{T,n}$ is the SU-Tx transmit power when activating the n-th port. To protect the QoS of primary networks, the SU-Tx applies the instantaneous power control [17] so that the interference power received at the PU is below a preset threshold I_{th}. Hence, when port n is active, the SU-Tx transmit power is

$$P_{T,n} = \min\left\{P_{\mathrm{tot}},\ \frac{I_{th}}{|h_{\mathrm{P},n}|^2}\right\}, \tag{1}$$

where P_{tot} denotes the maximum transmit power budget of the FA-enabled SU-Tx. The received signal sent from the n-th FA port of SU-Tx at the SU-Rx is given by

$$y_n = \sqrt{P_{T,n}} h_{\mathrm{S},n} s + g_n \tag{2}$$

where $g_n \sim \mathcal{CN}(0, N_0)$ denotes the AWGN, and $h_{S,n}$ denotes the complex channel gain between the n-th port and the SU-Rx. The corresponding signal-to-noise ratio (SNR) for decoding s takes the form

$$\gamma_n = \frac{P_{T,n}}{N_0}|h_{\mathrm{S},n}|^2 = \min\left\{\frac{P_{\mathrm{tot}}}{N_0}|h_{\mathrm{S},n}|^2,\ \frac{I_{th}|h_{\mathrm{S},n}|^2}{N_0|h_{\mathrm{P},n}|^2}\right\}. \tag{3}$$

The FA inter-port correlation is modeled by the correlation matrix $\boldsymbol{J} \in \mathbb{C}^{N\times N}$. Accordingly, the stacked channel vectors $\boldsymbol{h}_{\mathrm{S}} \triangleq [h_{\mathrm{S},1}, \ldots, h_{\mathrm{S},N}]^{\mathsf{T}}$ and $\boldsymbol{h}_{\mathrm{P}} \triangleq [h_{\mathrm{P},1}, \ldots, h_{\mathrm{P},N}]^{\mathsf{T}}$ take the following forms (cf. [2], [13], [15])

$$\boldsymbol{h}_{\mathrm{S}} = \sqrt{\mu_{\mathrm{S}}}\boldsymbol{J}^{\frac{1}{2}}\boldsymbol{z}, \quad \boldsymbol{h}_{\mathrm{P}} = \sqrt{\mu_{\mathrm{P}}}\boldsymbol{J}^{\frac{1}{2}}\boldsymbol{z}', \tag{4}$$

where $\boldsymbol{z}, \boldsymbol{z}' \sim \mathcal{CN}(\boldsymbol{0}_N, \boldsymbol{I}_N)$ are independent, and μ_{S} and μ_{P} capture the large-scale pathloss/shadowing of the SU-Tx–SU-Rx link and the SU-Tx–PU link respectively.

1) CR-Aware FA Port Selection: We propose a CR-aware FA port selection scheme that couples port choice with the underlay CR power-control mechanism as

$$n^*_{\mathrm{CR}} = \arg\max_{n\in[N]}\ \min\left\{\frac{P_{\mathrm{tot}}}{N_0}|h_{\mathrm{S},n}|^2,\ \frac{I_{th}|h_{\mathrm{S},n}|^2}{N_0|h_{\mathrm{P},n}|^2}\right\}, \tag{5}$$

and the resulting SNR is

$$\gamma_{\mathrm{CR}} = \max_{n\in[N]} \min\left\{\frac{P_{\mathrm{tot}}}{N_0}|h_{\mathrm{S},n}|^2,\ \frac{I_{th}|h_{\mathrm{S},n}|^2}{N_0|h_{\mathrm{P},n}|^2}\right\}. \tag{6}$$

2) Non-CR FA Port Selection: For comparison, we also consider the common FA port selection scheme in non-CR scenarios, where the FA port is selected with the maximum magnitude of the main channel between the SU-Tx and SU-Rx (cf. [2], [13], [15]), which we refer to the main channel maximization (MCM) FA port selection. The resulting SNR is given by

$$\gamma_{\mathrm{MCM}} = \min\left\{\frac{P_{\mathrm{tot}}}{N_0},\ \frac{I_{th}}{N_0|h_{\mathrm{P},n^*}|^2}\right\}\ \max_{n\in[N]}|h_{\mathrm{S},n}|^2, \tag{7}$$

where n^* is the index of the selected FA port, determined by

$$n^* = \arg\max_{n\in[N]}|h_{\mathrm{S},n}|^2. \tag{8}$$

[1]*Notation:* $\mathbb{C}$ denotes the set of complex numbers; $|\cdot|$ is the magnitude operator and $\|\cdot\|$ is the ℓ_2-norm; for a positive integer N, we write $[N] \triangleq \{1, 2, \ldots, N\}$; for a matrix $\boldsymbol{A}$, $\boldsymbol{A}^{\mathsf{T}}$, $\boldsymbol{A}^*$, and $\boldsymbol{A}^{\mathsf{H}}$ denote the transpose, element-wise conjugate, and conjugate transpose, respectively; $\mathbb{E}\{\cdot\}$ is the expectation operator; $\mathcal{CN}$ denotes the complex Gaussian distribution, and $\mathrm{Gamma}(m, \Omega)$ is the Gamma distribution with shape m and scale Ω; $\boldsymbol{0}_N$ is the $N \times 1$ zero vector, and $\boldsymbol{I}_N$ is the $N \times N$ identity matrix.

Since MCM selects the port solely via the SU link and is independent of the SU-Tx–PU channel [18], it follows that P_{T,n^*} is (statistically) independent of $\max_{n\in[N]}|h_{\mathrm{S},n}|^2$, and then $h_{\mathrm{P},n^*}\sim\mathcal{CN}(0,\mu_{\mathrm{P}})$.

3) Traditional Multi-Antenna Baseline: To compare with traditional antenna (TA) systems, we also consider that the SU-Tx is equipped with L TAs and employs the MRT scheme [19], where the transmit signal vector $\boldsymbol{s}\in\mathbb{C}^{L\times 1}$ is

$$\boldsymbol{s}=\sqrt{P_T}\frac{\boldsymbol{h}_{\mathrm{S,TA}}^*}{||\boldsymbol{h}_{\mathrm{S,TA}}||}s, \tag{9}$$

where P_T denotes the transmit power allocated to L antennas, and $\boldsymbol{h}_{\mathrm{S,TA}}\sim\mathcal{CN}(\boldsymbol{0}_L,\mu_{\mathrm{S}}\boldsymbol{I}_L)$ denotes the complex channel vector from the L transmit antennas to the SU-Rx. It is easy to check that

$$\mathbb{E}\{||\boldsymbol{s}||^2\}=P_T\mathbb{E}\left\{\frac{\boldsymbol{h}_{\mathrm{S,TA}}^{\mathsf{T}}\boldsymbol{h}_{\mathrm{S,TA}}^*}{||\boldsymbol{h}_{\mathrm{S,TA}}||^2}|s|^2\right\}=P_T. \tag{10}$$

Given the transmit signal design in (9), the interference power at the PU receiver is

$$I_{\mathrm{TA}}=P_T\left|\boldsymbol{h}_{\mathrm{P,TA}}^{\mathsf{T}}\frac{\boldsymbol{h}_{\mathrm{S,TA}}^*}{||\boldsymbol{h}_{\mathrm{S,TA}}||}\right|^2, \tag{11}$$

where $\boldsymbol{h}_{\mathrm{P,TA}}\sim\mathcal{CN}(\boldsymbol{0}_L,\mu_{\mathrm{P}}\boldsymbol{I}_L)$ denotes the complex channel vector from the L transmit antennas to the PU receiver. As $\boldsymbol{h}_{\mathrm{S,TA}}$ and $\boldsymbol{h}_{\mathrm{P,TA}}$ are independent, we have

$$h'_{\mathrm{P,TA}}\triangleq\boldsymbol{h}_{\mathrm{P,TA}}^{\mathsf{T}}\frac{\boldsymbol{h}_{\mathrm{S,TA}}^*}{||\boldsymbol{h}_{\mathrm{S,TA}}||}\sim\mathcal{CN}(0,\mu_{\mathrm{P}}). \tag{12}$$

Thus, the power control at the SU-Tx in the traditional multi-antenna setting takes the form

$$P_T=\min\left\{P_{\mathrm{tot}},\ \frac{I_{th}}{|h'_{\mathrm{P,TA}}|^2}\right\}. \tag{13}$$

The resulting SNR at the SU-Rx is of the form

$$\gamma_{\mathrm{TA}}=\min\left\{\frac{P_{\mathrm{tot}}}{N_0},\ \frac{I_{th}}{N_0|h'_{\mathrm{P,TA}}|^2}\right\}||\boldsymbol{h}_{\mathrm{S,TA}}||^2. \tag{14}$$

III. Diversity Order Analysis

This section will establish the exact diversity orders of the considered schemes under correlated Rayleigh fading with FA-port correlation captured by the matrix $\boldsymbol{J}$ with rank of M. We adopt the cmmon high-quality main-channel regime of the SU-Tx–SU-Rx link (equivalently, $\mu_{\mathrm{S}}\to\infty$) [17], [20]. Results are presented for the baseline MCM, the proposed CR-aware selection, and the TA benchmark with MRT.

The diversity order of the secondary network is defined as

$$D\triangleq\lim_{\mu_{\mathrm{S}}\to\infty}-\frac{\ln \mathrm{OP}}{\ln\mu_{\mathrm{S}}}, \tag{15}$$

where OP denotes the outage probability at the SU-Rx with an SNR threshold γ_{th}.

We first have the SNR comparison between CR-aware and non-CR port selection schemes.

Theorem 1: For the instantaneous SNRs at the SU-Rx under the CR-aware and MCM FA port selection schemes in the underlay CR networks, we always have

$$\gamma_{\mathrm{CR}}\geq\gamma_{\mathrm{MCM}}. \tag{16}$$

Proof: We recall that n^* is the port index selected by MCM (cf. (8)). Using the SNR expression of γ_{CR} in (6), we have

$$\begin{aligned}\gamma_{\mathrm{CR}}&=\max_{n\in[N]}\min\left\{\frac{P_{\mathrm{tot}}}{N_0}|h_{\mathrm{S},n}|^2,\ \frac{I_{th}|h_{\mathrm{S},n}|^2}{N_0|h_{\mathrm{P},n}|^2}\right\}\\&\geq\min\left\{\frac{P_{\mathrm{tot}}}{N_0}|h_{\mathrm{S},n^*}|^2,\ \frac{I_{th}|h_{\mathrm{S},n^*}|^2}{N_0|h_{\mathrm{P},n^*}|^2}\right\}\\&=\frac{P_{T,n^*}}{N_0}\max_{n\in[N]}|h_{\mathrm{S},n}|^2=\gamma_{\mathrm{MCM}},\end{aligned} \tag{17}$$

which leads to Theorem 1. ■

We now state the diversity order of MCM port selection.

Theorem 2: The diversity order under the MCM FA port selection scheme is the rank of the correlation matrix $\boldsymbol{J}$, i.e., $D_{\mathrm{MCM}}=\mathrm{Rank}\{\boldsymbol{J}\}=M$.

Proof: We begin by establishing bounds on $\max_{n\in[N]}|h_{\mathrm{S},n}|^2$ as follows

$$\frac{1}{N}\sum_{n=1}^{N}|h_{\mathrm{S},n}|^2\leq\max_{n\in[N]}|h_{\mathrm{S},n}|^2\leq\sum_{n=1}^{N}|h_{\mathrm{S},n}|^2=||\boldsymbol{h}_{\mathrm{S}}||^2. \tag{18}$$

In view of (4), we can rewrite $||\boldsymbol{h}_{\mathrm{S}}||^2$ as

$$\begin{aligned}||\boldsymbol{h}_{\mathrm{S}}||^2&=\boldsymbol{h}_{\mathrm{S}}^{\mathsf{H}}\boldsymbol{h}_{\mathrm{S}}=\mu_{\mathrm{S}}\ \boldsymbol{z}^{\mathsf{H}}\boldsymbol{J}\boldsymbol{z}\\&\overset{(a)}{=}\mu_{\mathrm{S}}\ \boldsymbol{z}^{\mathsf{H}}\boldsymbol{U}\boldsymbol{\Lambda}\boldsymbol{U}^{\mathsf{H}}\boldsymbol{z}=\mu_{\mathrm{S}}\sum_{n=1}^{M}\lambda_n\left|\left[\boldsymbol{U}^{\mathsf{H}}\boldsymbol{z}\right]_n\right|^2,\end{aligned} \tag{19}$$

where step (a) follows from the eigenvalue decomposition of $\boldsymbol{J}$, λ_n denotes the n-th largest *non-zero* eigenvalue of $\boldsymbol{J}$, and $\left[\boldsymbol{U}^{\mathsf{H}}\boldsymbol{z}\right]_n$ denotes the n-th element of the vector $\boldsymbol{U}^{\mathsf{H}}\boldsymbol{z}$. As $\boldsymbol{U}$ is an unitary matrix, for $\boldsymbol{U}^{\mathsf{H}}\boldsymbol{z}$, we have

$$\mathbb{E}\left\{\left(\boldsymbol{U}^{\mathsf{H}}\boldsymbol{z}\right)\left(\boldsymbol{U}^{\mathsf{H}}\boldsymbol{z}\right)^{\mathsf{H}}\right\}=\boldsymbol{U}^{\mathsf{H}}\mathbb{E}\left\{\boldsymbol{z}\boldsymbol{z}^{\mathsf{H}}\right\}\boldsymbol{U}=\boldsymbol{I}_N, \tag{20}$$

which implies that $\boldsymbol{U}^{\mathsf{H}}\boldsymbol{z}\sim\mathcal{CN}(\boldsymbol{0}_N,\boldsymbol{I}_N)$, and consequently, $\left|\left[\boldsymbol{U}^{\mathsf{H}}\boldsymbol{z}\right]_n\right|^2$ is an exponentially distributed random variable with unit mean. Define $X\triangleq\sum_{n=1}^{M}\left|\left[\boldsymbol{U}^{\mathsf{H}}\boldsymbol{z}\right]_n\right|^2$, which is the sum of M i.i.d. exponentially random variables. Thus, X follows from a Gamma distribution with shape parameter M and unit scale parameter, and the cumulative distribution function (CDF) of X takes the form [16]

$$F_X(x)=\frac{1}{\Gamma(M)}\Upsilon(M,x)\overset{x\to 0}{\simeq}\frac{x^M}{M\Gamma(M)}+o(x^M), \tag{21}$$

where $\Gamma(\cdot)$ and $\Upsilon(\cdot,\cdot)$ denote the Gamma function and the lower incomplete Gamma function [21], respectively.

Based on (19), we have bounds for $||\boldsymbol{h}_{\mathrm{S}}||^2$ as

$$\mu_{\mathrm{S}}\lambda_{\min}X\leq||\boldsymbol{h}_{\mathrm{S}}||^2\leq\mu_{\mathrm{S}}\lambda_{\max}X \tag{22}$$

where $\lambda_{\min}$ and $\lambda_{\max}$ denote the minimum and maximum non-zero eigenvalues of $\boldsymbol{J}$, respectively. By combining (22) with (18), we obtain bounds on $\max_{n\in[N]}|h_{\mathrm{S},n}|^2$ as follows

$$\frac{1}{N}\mu_{\mathrm{S}}\lambda_{\min}X \le \max_{n\in[N]}|h_{\mathrm{S},n}|^2 \le \mu_{\mathrm{S}}\lambda_{\max}X, \tag{23}$$

which leads to the bounds for OP of MCM selection as

$$\Pr\left\{X \le \frac{\gamma_{th}N_0}{\mu_{\mathrm{S}}\lambda_{\max}P_{T,n^*}}\right\} \le \mathrm{OP}_{\mathrm{MCM}} \le \Pr\left\{X \le \frac{\gamma_{th}NN_0}{\mu_{\mathrm{S}}\lambda_{\min}P_{T,n^*}}\right\}. \tag{24}$$

As $\mu_{\mathrm{S}} \to \infty$, using the asymptotic CDF of X in (21), we have the asymptotic result

$$\Pr\left\{X \le \frac{\gamma_{th}N_0}{\mu_{\mathrm{S}}\lambda_{\max}P_{T,n^*}}\right\} \simeq \frac{\mu_{\mathrm{S}}^{-M}}{M\Gamma(M)}\mathbb{E}_{P_{T,n^*}}\left\{\left(\frac{\gamma_{th}N_0}{\lambda_{\max}P_{T,n^*}}\right)^M\right\} + o(\mu_{\mathrm{S}}^{-M}), \tag{25}$$

which leads to

$$\lim_{\mu_{\mathrm{S}}\to\infty} -\frac{\ln\Pr\left\{X \le \frac{\gamma_{th}N_0}{\mu_{\mathrm{S}}\lambda_{\max}P_{T,n^*}}\right\}}{\ln\mu_{\mathrm{S}}} = M. \tag{26}$$

Similarly, we can obtain

$$\lim_{\mu_{\mathrm{S}}\to\infty} -\frac{\ln\Pr\left\{X \le \frac{\gamma_{th}NN_0}{\mu_{\mathrm{S}}\lambda_{\min}P_{T,n^*}}\right\}}{\ln\mu_{\mathrm{S}}} = M. \tag{27}$$

Combining (26), (27) and (24) and considering the Squeeze Theorem, we finally derive

$$\lim_{\mu_{\mathrm{S}}\to\infty} -\frac{\ln\mathrm{OP}_{\mathrm{MCM}}}{\ln\mu_{\mathrm{S}}} = M, \tag{28}$$

which completes the proof. ■

In the following, we present the diversity order of the CR-aware port selection policy.

Theorem 3: The diversity order of the CR-aware FA port selection equals the rank of the correlation matrix $\boldsymbol{J}$, i.e., $D_{\mathrm{CR}} = \mathrm{Rank}\{\boldsymbol{J}\} = M$.

Proof: Given the SNR expression in (6), we first have the upper bound for γ_{CR} as

$$\gamma_{\mathrm{CR}} \le \max_{n\in[N]}\frac{P_{\mathrm{tot}}}{N_0}|h_{\mathrm{S},n}|^2 \triangleq \gamma_{\mathrm{up}}. \tag{29}$$

So the OP of CR-aware port selection is lower bounded by

$$\mathrm{OP}_{\mathrm{CR}} = \Pr\{\gamma_{\mathrm{CR}} \le \gamma_{th}\} \ge \mathrm{P}_{\mathrm{out}}^{\mathrm{low}} \triangleq \Pr\{\gamma_{\mathrm{up}} \le \gamma_{th}\}. \tag{30}$$

In view of [16, Thm. 1], we know that

$$\lim_{\mu_S\to\infty} -\frac{\ln\mathrm{P}_{\mathrm{out}}^{\mathrm{low}}}{\ln\mu_S} = M. \tag{31}$$

Invoking Theorem 1, we obtain the following upper bound on $\mathrm{OP}_{\mathrm{CR}}$ as

$$\mathrm{OP}_{\mathrm{CR}} \le \mathrm{OP}_{\mathrm{MCM}}, \tag{32}$$

which implies that

$$D_{\mathrm{CR}} \ge D_{\mathrm{MCM}} \triangleq \lim_{\mu_{\mathrm{S}}\to\infty} -\frac{\ln\mathrm{OP}_{\mathrm{MCM}}}{\ln\mu_{\mathrm{S}}}. \tag{33}$$

Putting (33), (31), and (28) together and applying the Squeeze Theorem, we conclude that

$$\lim_{\mu_{\mathrm{S}}\to\infty} -\frac{\ln\mathrm{OP}_{\mathrm{CR}}}{\ln\mu_{\mathrm{S}}} = M, \tag{34}$$

which concludes the proof. ■

Remark 1: We adopt a method similar to our latest work [16], which analyzed the diversity order of FA systems in a non-CR P2P setting, to *rigorously* establish the exact diversity order in the underlay CR scenario considered here. This departs from the classical approach that first derives a closed-form OP and then evaluates the limit in (15) to derive the diversity order. For FA with spatially correlated ports, an exact closed-form OP is not available; existing closed-form OP expressions even for P2P are approximation-based (e.g., [13]–[15]), from which the exact diversity order cannot, in general, be rigorously inferred.

Remark 2: Both FA selection strategies—MCM and CR-aware—exhibit the same diversity order, governed by $\mathrm{Rank}\{\boldsymbol{J}\}$. Coupled with the earlier dominance result ($\gamma_{\mathrm{CR}} \ge \gamma_{\mathrm{MCM}}$), this implies that CR-aware never reduces reliability relative to MCM and typically yields lower outage at finite SNR, while the asymptotic slope is dictated solely by spatial correlation. These behaviors are also corroborated by the numerical results in Figs. 1–3.

For completeness, we also derive the diversity order of the traditional multi-antenna benchmark.

Theorem 4: Under a traditional MRT scheme with L antennas at the SU-Tx, the diversity order equals L.

Proof: Since $\boldsymbol{h}_{\mathrm{S,TA}} \sim \mathcal{CN}(\boldsymbol{0}L, \mu_{\mathrm{S}}\boldsymbol{I}_L)$, its entries are i.i.d. $\mathcal{CN}(0,\mu_{\mathrm{S}})$, so the squared magnitudes are i.i.d. exponential random variables with mean μ_{S}. Since $\|\boldsymbol{h}_{\mathrm{S,TA}}\|^2$ equals the sum of the squared magnitudes of the entries of $\boldsymbol{h}_{\mathrm{S,TA}}$, it follows that $\|\boldsymbol{h}_{\mathrm{S,TA}}\|^2 \sim \mathrm{Gamma}(L,\mu_{\mathrm{S}})$. which means that the asymptotic CDF of $||\boldsymbol{h}_{\mathrm{S,TA}}||^2$ is of the form

$$F_{||\boldsymbol{h}_{\mathrm{S,TA}}||^2}(x) \overset{\mu_{\mathrm{S}}\to\infty}{\simeq} \frac{x^L\mu_{\mathrm{S}}^{-L}}{L\Gamma(L)} + o(\mu_{\mathrm{S}}^{-L}). \tag{35}$$

Using the SNR expression in (14), the asymptotic OP of the traditional multi-antenna MRT scheme is obtained as

$$\begin{aligned}\mathrm{OP}_{\mathrm{TA}} &= \Pr\left\{||\boldsymbol{h}_{\mathrm{S,TA}}||^2 \le \frac{N_0\gamma_{th}}{P_T}\right\} \\ &= \mathbb{E}_{P_T}\left\{F_{||\boldsymbol{h}_{\mathrm{S,TA}}||^2}\left(\frac{N_0\gamma_{th}}{P_T}\right)\right\} \\ &\overset{(a)}{\simeq} \mu_{\mathrm{S}}^{-L}\ \mathbb{E}_{P_T}\left\{\left(\frac{N_0\gamma_{th}}{P_T}\right)^L\frac{1}{L\Gamma(L)}\right\},\end{aligned} \tag{36}$$

where step (a) follows from using (35). Finally, we have

$$\lim_{\mu_{\mathrm{S}}\to\infty} -\frac{\ln\mathrm{OP}_{\mathrm{TA}}}{\ln\mu_{\mathrm{S}}} = L, \tag{37}$$

which completes the proof. ■

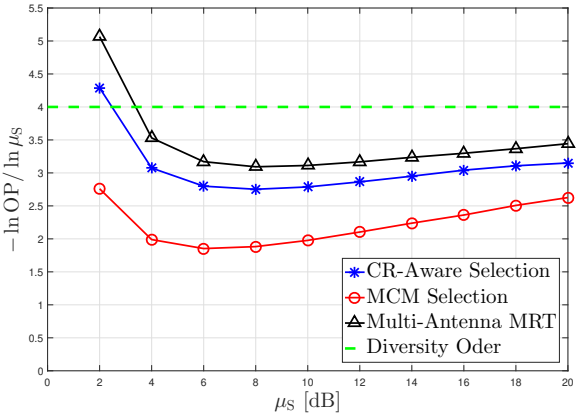

Fig. 1: Effective diversity order versus μ_{S} for $W = 1$, $N = L = 4$, $N_0 = 1$, $P_{\mathrm{tot}} = 2I_{th} = 10$ dB, $\gamma_{th} = 5$ and $\mu_{\mathrm{P}} = 2$

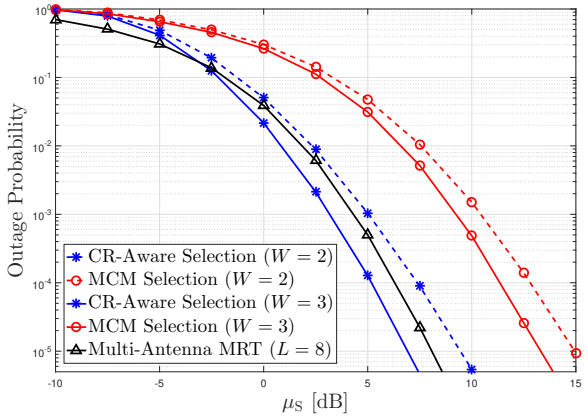

Fig. 2: Outage probability versus μ_{S} for $N = 16$, $P_{\mathrm{tot}} = 2I_{th} = 10$ dB, $\gamma_{th} = 5$, $N_0 = 1$ and $\mu_{\mathrm{P}} = 2$

IV. Numerical Results

In this section, we present numerical results to validate the analytical model and to quantify the performance advantages of the proposed CR-aware FA port selection over the non-CR MCM policy and a traditional multi-antenna MRT benchmark. The SU-Tx adopts a linear FA with N ports. Spatial correlation among FA ports is the widely used Jake's model [2], where the (m, n)-th entry of $\boldsymbol{J}$ takes the form

$$[\boldsymbol{J}]_{m,n} = J_0\left(2\pi \frac{(m-n)}{N-1} W\right), \tag{38}$$

in which $J_0(\cdot)$ denotes the zeroth-order Bessel function of the first kind [21], and W is the FA length normalized to the carrier wavelength.

Fig. 1 plots the empirical effective diversity order, $-\ln(\mathrm{OP})/\ln(\mu_S)$, versus μ_S for three schemes: CR-aware FA port selection (single RF chain), MCM FA port selection (single RF chain), and the TA benchmark with MRT (L RF chains). With $W = 1$ and $N = 4$, we have $M = \mathrm{Rank}\{\boldsymbol{J}\} = N$; together with the TA benchmark using $L = 4$ antennas, this yields the reference line $-\ln(\mathrm{OP})/\ln(\mu_S) = 4$, indicating the diversity orders of both FA and TA systems as established by Theorems 2–4. As μ_S increases, all curves exhibit a two-stage evolution—an initial sharp drop at small μ_S followed by a gradual rise—and ultimately approach the reference line of $-\ln(\mathrm{OP})/\ln(\mu_S) = 4$. This convergence trend confirms Theorems 2–4. Over the practically relevant finite-μ_S range, the distance to the reference line differs across schemes: TA-MRT remains the closest, CR-aware selection is intermediate, and MCM is the farthest. This ordering mirrors the observed outage performance: TA-MRT benefits from coherent combining with $L = 4$ RF chains; the CR-aware rule couples port selection with the underlay power-control mechanism jointly with the main-channel quality; whereas MCM relies solely on the main-channel gain and ignores the power-control link during selection.

Fig. 2 plots the OP versus μ_{S} for three schemes: CR-aware FA port selection and MCM FA port selection—each evaluated under two FA lengths, $W = 2$ and $W = 3$ with $N = 16$ ports—and the TA benchmark with MRT using $L = 8$ antennas. As μ_{S} increases, all curves decrease monotonically, reflecting improvement of the main channel between the SU-Tx and the SU-Rx. Notably, the CR-aware FA with $W = 3$ outperforms TA-MRT ($L = 8$) in the medium-to-high μ_{S} range. Although TA-MRT yields a lower OP than CR-aware FA at very small μ_{S}, those operating points typically correspond to OP well above 0.1, which is of limited practical relevance for reliable communications. The MCM policy is consistently the weakest across the sweep; increasing the FA length from $W = 2$ to $W = 3$ reduces its OP but does not surpass the TA-MRT benchmark.

Fig. 3 plots the OP versus the interference threshold I_{th}—which determines the underlay power cap at the SU-Tx—for three schemes: CR-aware FA port selection, MCM FA port selection, and the TA-MRT benchmark with $L = 4$ antennas. As I_{th} increases, all curves decrease steadily and then flatten once I_{th} becomes sufficiently large. This flattening occurs because a very large I_{th} effectively deactivates the underlay constraint, reducing the setup to a non-CR case; in that regime, CR-aware and MCM reduce to the same rule and their OP curves merge. In the low-to-medium I_{th} range, the CR-aware policy with $N = 6$ achieves a lower OP than TA-MRT ($L = 4$); at very large I_{th}, where the system behaves as non-CR, TA-MRT becomes superior. The OP of MCM remains above the TA-MRT benchmark for $N = 6$ and $N = 24$ in the low-to-medium I_{th} regime; notably, with $N = 24$, MCM eventually outperforms TA-MRT once I_{th} is large enough. Finally, although [13, Table II] (non-CR, $W = 2$) reports negligible OP improvement beyond 6 ports, Fig. 3 shows that under underlay CR increasing the port count to $N = 24$ (still $W = 2$) yields a clear OP reduction for both FA selection schemes. This highlights a CR-specific advantage: underlay power control tied to the interference link introduces additional selection variability across ports (through their different coupling to the PU), so enlarging the port set offers more chances to select ports for which

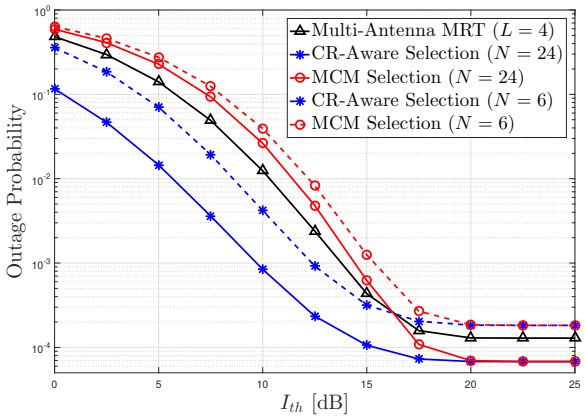

Fig. 3: Outage probability versus I_{th} for $W = 2$, $P_{\text{tot}} = 10$ dB, $\gamma_{th} = 5$, $N_0 = 1$ and $\mu_{\text{S}} = \mu_{\text{P}} = 2$

the SU-Tx transmit power—dynamically adjusted via the PU interference link—becomes higher, an effect that is absent in the non-CR setting.

V. Conclusion and Discussions

We studied FA port selection in underlay CR and proposed a CR-aware rule that couples port choice with the underlay power-control mechanism. Via rigorous proofs, we established that the diversity orders of both CR-aware selection and MCM equal the rank of the FA port correlation matrix, while a traditional multi-antenna transmitter with MRT achieves a diversity order equal to the number of transmit antennas; moreover, the instantaneous SNR under CR-aware selection is proved to always dominate that under MCM.

Numerical results corroborate and quantify these insights. The effective diversity order curves converge to the limit stated in Theorems 2–4. With $N = 16$, increasing the FA length from $W = 2$ to $W = 3$ reduces outage and allows CR-aware selection to surpass an $L = 8$ MRT benchmark in the medium-to-high μ_{S} range; by contrast, operating points where MRT is better typically correspond to OP well above 0.1. When sweeping I_{th}, all schemes improve and then saturate; in the low-to-medium I_{th} regime, CR-aware with $N = 6$ outperforms MRT with $L = 4$, while at very large I_{th} the setting effectively becomes non-CR and MRT is superior. Finally, under underlay CR, raising the *saturation* FA port count (e.g., for $W = 2$: $N = 6 \to 24$) yields sizeable OP gains beyond the non-CR saturation count, indicating that underlay power control expands the port-selection freedom.

Regarding practical considerations, CR-aware selection requires the SU–PU channel information for all N ports, whereas MCM only needs this information for the single port selected from the SU link. However, both schemes rely on channel variations to trigger port switching, so the switching burden remains comparable to that of non-CR FA systems. Moreover, due to the strong spatial correlation among FA ports, the SU–PU channels of most ports can be inferred from only a few measurements, making the resulting overhead of CR-aware selection mild—particularly for low-mobility users, where the wireless channel varies slowly over time.

References

[1] K.-K. Wong, A. Shojaeifard, K.-F. Tong, and Y. Zhang, "Fluid antenna systems," *IEEE Trans. Wireless Commun.*, vol. 20, no. 3, pp. 1950–1962, Mar. 2021.

[2] K.-K. Wong, W. K. New, X. Hao, K.-F. Tong, and C.-B. Chae, "Fluid antenna system—part I: Preliminaries," *IEEE Commun. Lett.*, vol. 27, no. 8, pp. 1919–1923, Aug. 2023.

[3] K.-K. Wong, K.-F. Tong, Y. Shen, Y. Chen, and Y. Zhang, "Bruce lee-inspired fluid antenna system: Six research topics and the potentials for 6G," *Frontiers Commun. Netw.*, vol. 3, p. 853416, Mar. 2022.

[4] K.-F. Tong, B. Liu, and K.-K. Wong, "Designs and challenges in fluid antenna system hardware," *Electronics*, vol. 14, no. 7, 2025.

[5] A. Ali and W. Hamouda, "Advances on spectrum sensing for cognitive radio networks: Theory and applications," *IEEE Commun. Surv. Tutor.*, vol. 19, no. 2, pp. 1277–1304, 2017.

[6] D. H. Tashman and W. Hamouda, "An overview and future directions on physical-layer security for cognitive radio networks," *IEEE Network*, vol. 35, no. 3, pp. 205–211, 2021.

[7] A. Ahmad, S. Ahmad, M. H. Rehmani, and N. U. Hassan, "A survey on radio resource allocation in cognitive radio sensor networks," *IEEE Commun. Surv. Tutor.*, vol. 17, no. 2, pp. 888–917, 2015.

[8] J. Yao, M. Jin, T. Wu, M. Elkashlan, C. Yuen, K.-K. Wong, G. K. Karagiannidis, and H. Shin, "FAS-driven spectrum sensing for cognitive radio networks," *IEEE Internet Things J.*, vol. 12, no. 5, pp. 6046–6049, Mar. 2025.

[9] L. Tlebaldiyeva, S. Arzykulov, A.-A. A. Boulogeorgos, T. A. Tsiftsis, and G. Nauryzbayev, "Fluid antenna wireless systems for enhanced spectrum sensing," in *Proc. IEEE Globecom Workshops (GC Wkshps)*, 2024, pp. 1–5.

[10] M. Chitra, S. Yashaswini, and S. Dhanasekaran, "Performance analysis of cooperative underlay NOMA-assisted cognitive radio networks," *IEEE Wireless Commun. Lett.*, vol. 13, no. 1, pp. 203–207, Jan. 2024.

[11] S. Thakur and A. Singh, "Underlay cognitive radio with instantaneous interference constraint: A secrecy performance," *IEEE Trans. Veh. Technol.*, vol. 70, no. 8, pp. 7839–7844, Aug. 2021.

[12] B. Li, J. Park, and J. Choi, "On optimal power control for cognitive satellite-terrestrial systems," *IEEE Wireless Commun. Lett.*, vol. 13, no. 10, pp. 2737–2741, Oct. 2024.

[13] W. K. New, K.-K. Wong, H. Xu, K.-F. Tong and C.-B. Chae, "Fluid antenna system: New insights on outage probability and diversity gain," *IEEE Trans. Wireless Commun.*, vol. 23, no. 1, pp. 128–140, Jan. 2024.

[14] J. D. Vega-Sánchez, A. E. López-Ramírez, L. Urquiza-Aguiar, and D. P. M. Osorio, "Novel expressions for the outage probability and diversity gains in fluid antenna system," *IEEE Wireless Commun. Lett.*, vol. 13, no. 2, pp. 372–376, Feb. 2024.

[15] M. Khammassi, A. Kammoun, and M.-S. Alouini, "A new analytical approximation of the fluid antenna system channel," *IEEE Trans. Wireless Commun.*, vol. 22, no. 12, pp. 8843–8858, Dec. 2023.

[16] H. Zhao and D. Slock, "Analytical insights into outage probability and ergodic capacity of fluid antenna systems," *IEEE Wireless Commun. Lett.*, vol. 14, no. 5, pp. 1581–1585, May 2025.

[17] H. Zhao, J. Zhang, L. Yang, G. Pan, and M.-S. Alouini, "Secure mmWave communications in cognitive radio networks," *IEEE Wireless Commun. Lett.*, vol. 8, no. 4, pp. 1171–1174, Aug. 2019.

[18] H. Zhao, Y. Tan, G. Pan, Y. Chen, and N. Yang, "Secrecy outage on transmit antenna selection/maximal ratio combining in MIMO cognitive radio networks," *IEEE Trans. Veh. Technol.*, vol. 65, no. 12, pp. 10 236–10 242, Dec. 2016.

[19] H. Zhao, D. Slock, and P. Elia, "Exact SINR analysis of matched-filter precoder," in *Proc. 25th IEEE Int. Workshop Signal Process. Adv. Wireless Commun. (SPAWC)*, Sep. 2024, pp. 901–905.

[20] S. Yadav, "Secrecy performance of cognitive radio sensor networks over $\alpha - \mu$ fading channels," *IEEE Sensors Lett.*, vol. 4, no. 9, pp. 1–4, Sep. 2020.

[21] I. S. Gradshteyn and I. M. Ryzhik, *Table of integrals, series, and products*, 7th ed. Academic press, 2007.